GEOLOGY | THE GEOLOGICAL SOCIETY OF AMERICA®

https://doi.org/10.1130/G46367.1

Manuscript received 10 April 2019
Revised manuscript received 21 June 2019
Manuscript accepted 26 June 2019

Published online 16 July 2019

Mixed deformation styles observed on a shallow subduction thrust, Hikurangi margin, New Zealand

Å. Fagereng[1], H.M. Savage[2], J.K. Morgan[3], M. Wang[4], F. Meneghini[5], P.M. Barnes[6], R. Bell[7], H. Kitajima[8], D.D. McNamara[9], D.M. Saffer[10], L.M. Wallace[11], K. Petronotis[12], L. LeVay[12], and the IODP Expedition 372/375 Scientists*
[1]School of Earth & Ocean Sciences, Cardiff University, Cardiff CF10 3AT, UK
[2]Lamont-Doherty Earth Observatory, Columbia University, Palisades, New York 10964, USA
[3]Department of Earth Science, Rice University, Houston, Texas 77005, USA
[4]College of Oceanography, Hohai University, Nanjing, Jiangsu 210093, China
[5]Dipartimento di Scienze della Terra, Universita degli Studi di Pisa, Pisa 56126, Italy
[6]National Institute of Water and Atmospheric Research, Wellington 6021, New Zealand
[7]Basins Research Group, Imperial College London, Kensington SW7 2AZ, UK
[8]Department of Geology and Geophysics, Texas A&M University, College Station, Texas 77845, USA
[9]Department of Earth, Ocean and Ecological Sciences, University of Liverpool, Liverpool L69 3GP, UK
[10]Department of Geosciences, The Pennsylvania State University, University Park, Pennsylvania 16802, USA
[11]GNS Science, Lower Hutt 5040, New Zealand
[12]International Ocean Discovery Program, Texas A&M University, College Station, Texas 77845, USA

ABSTRACT

Geophysical observations show spatial and temporal variations in fault slip style on shallow subduction thrust faults, but geological signatures and underlying deformation processes remain poorly understood. International Ocean Discovery Program (IODP) Expeditions 372 and 375 investigated New Zealand's Hikurangi margin in a region that has experienced both tsunami earthquakes and repeated slow-slip events. We report direct observations from cores that sampled the active Pāpaku splay fault at 304 m below the seafloor. This fault roots into the plate interface and comprises an 18-m-thick main fault underlain by ~30 m of less intensely deformed footwall and an ~10-m-thick subsidiary fault above undeformed footwall. Fault zone structures include breccias, folds, and asymmetric clasts within transposed and/or dismembered, relatively homogeneous, silty hemipelagic sediments. The data demonstrate that the fault has experienced both ductile and brittle deformation. This structural variation indicates that a range of local slip speeds can occur along shallow faults, and they are controlled by temporal, potentially far-field, changes in strain rate or effective stress.

INTRODUCTION

The shallow portion of subduction thrust faults, between the trench and the seismogenic zone, can slip in a variety of modes, including steady creep, slow-slip events (SSEs), afterslip, and coseismic slip (Saffer and Wallace, 2015; Araki et al., 2017). Understanding how these shallow regions accommodate displacement is critical for making estimates of potential earthquake magnitude and tsunami forecasts. Three existing hypotheses seek to explain temporal and spatial variations in fault slip style: (1) contrasting material properties within the fault zone give rise to mixed behavior (Skarbek et al., 2012; Webber et al., 2018); (2) perturbations to fault stability occur through changes in loading rate (Scholz, 1998; Ikari and Kopf, 2017; Leeman et al., 2018); and (3) low effective stresses promote transitional frictional stability (Liu and Rice, 2007; Segall et al., 2010). Direct observation of fault zone materials is necessary to evaluate these hypotheses.

International Ocean Discovery Program (IODP) Expeditions 372 and 375 drilled, logged, and sampled the Pāpaku thrust at Site U1518 offshore New Zealand's North Island (Fig. 1). This is a major, and highly active, splay fault rooted in the Hikurangi margin plate interface. Here, we describe this shallow subduction fault and discuss spatial and temporal variability in fault slip style.

TECTONIC SETTING OF THE PĀPAKU FAULT

In the area of drilling, the Pacific plate is subducting beneath the Australian plate at a rate of ~5.5 cm/yr (Fig. 1A; Wallace et al., 2004). Large portions of the offshore northern Hikurangi margin slip in SSEs, with small intervening patches of interseismic locking. SSEs repeat every 18–24 mo, last a few weeks, and are interpreted to accommodate ~5–25 cm of slip on the plate interface (Wallace and Beavan, 2010; Wallace et al., 2016). A recent study using seafloor absolute pressure gauges suggested that SSEs propagate to within ≤2 km of the seafloor (Wallace et al., 2016). The data cannot differentiate whether slow slip near the deformation front is limited to the deeper plate interface or also includes slip along splay faults within the prism. Burst-type repeating earthquakes along upper-plate faults coincide with tremor events after northern Hikurangi SSEs, consistent with

*International Ocean Discovery Program, Hikurangi Subduction Margin, 26 November 2017–4 January 2018 and 8 March–5 May 2018; see the GSA Data Repository[1] for list of participants.

[1]GSA Data Repository item 2019315, list of participants in IODP Expeditions 372/375 and Figures DR1–DR5, is available online at http://www.geosociety.org/datarepository/2019/, or on request from editing@geosociety.org.

CITATION: Fagereng, Å., et al., 2019, Mixed deformation styles observed on a shallow subduction thrust, Hikurangi margin, New Zealand: Geology, v. 47, p. 872–876, https://doi.org/10.1130/G46367.1

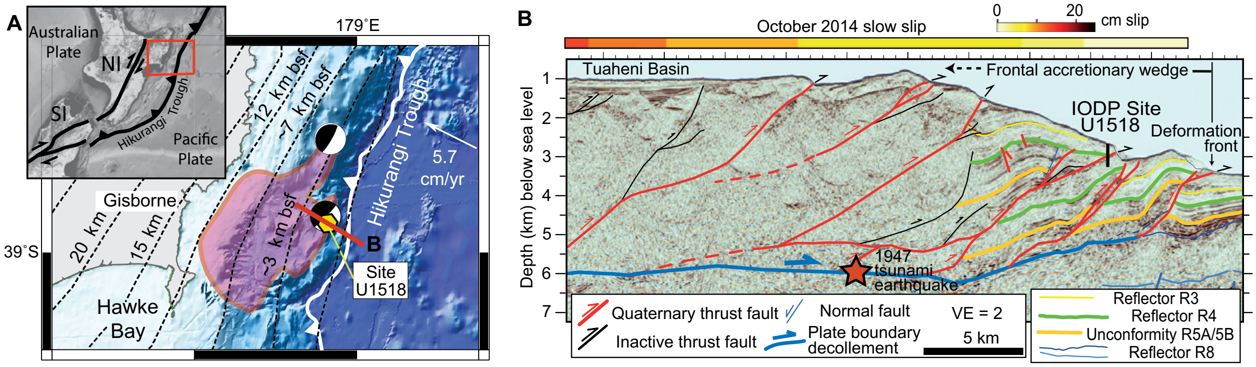

Figure 1. (A) Map of the northern Hikurangi subduction margin, New Zealand. Shaded pink area shows slip extent from the September–October 2014 slow slip event (SSE; Wallace et al., 2016). Focal mechanisms show hypocenters of C.E. 1947 tsunami earthquakes (Doser and Webb, 2003). Yellow hexagon is location of International Ocean Discovery Program (IODP) Expedition 375 Site 1518. Red line is location of seismic section in B. Inset shows map area. NI—North Island; SI—South Island; bsf—below seafloor. (B) Seismic section converted to depth using stacking velocities (high-density velocity model of Barker et al. [2018]), showing interpreted major faults, selected pre-expedition seismic reflection stratigraphy, drill site U1518, location of March 1947 tsunami earthquake (Bell et al., 2014), and distribution of slow slip during the 2014 SSE (Wallace et al., 2016). VE—vertical exaggeration.

splay faults being involved in SSEs (Shaddox and Schwartz, 2019).

The Pāpaku thrust dips ≤30°W within the narrow accretionary prism, 6.5 km west of the deformation front (Fig. 1; Wallace et al., 2019). It roots into the plate interface 10–25 km landward of the drill site, within or immediately above the SSE zone (Wallace et al., 2016; Barker et al., 2018), and near or within the rupture area of two M_w 6.9–7.1 (C.E. 1947) tsunami earthquakes (Fig. 1; Doser and Webb, 2003; Bell et al., 2014). The fault cuts through the middle of its scarp in an area of localized landslides where seismic interpretation indicates ~6 km of dip-slip displacement on the fault (Fig. 1B). We interpret this bathymetric relief and large displacement to indicate recent activity, as is also suggested based on short-lived geochemical signatures preserved in interstitial waters in the hanging wall and footwall (Solomon et al., 2018). Although it is currently unknown whether the Pāpaku fault hosts SSEs, it provides a unique natural laboratory in which to directly observe fault zone structure in an area where both SSEs and tsunami earthquakes are known to occur at shallow depths.

FAULT ZONE ARCHITECTURE

Core recovery through the Pāpaku fault zone was ~33% (Fig. 2), comparable to other subduction zone fault drilling (Kinoshita et al., 2009; Screaton et al., 2009; Chester et al., 2013). The fault zone contains brittle and ductile features in Pleistocene hemipelagic sediments. We define "brittle" as discrete faults and fractures (Fig. 3A), and zones of macroscopically discontinuous deformation, such as breccias that disrupt layering (Fig. 3B). "Ductile" is a descriptive term for intervals of dismembered layering that are inferred to record macroscopic flow, commonly with asymmetry indicating shear (Figs. 3C–3F). Layer-parallel ductile extension is also interpreted from pinch-and-swell structures, and dismembered layering where clasts are not markedly asymmetric (Fig. 3G). These latter features resemble stratal disruption, which typically implies tectonic modification in this setting (e.g., Byrne, 1984; Maltman, 1998). We grouped all structures inferred to record layer-parallel, macroscopic flow as "flow banding," as we could not confidently separate components of pure and simple shear. This flow banding is distinguished from gravitational mass transport deposits (MTDs), which are common in the footwall but are characterized by overlying upward-fining sediments and a chaotic internal fabric above an erosional base (Strasser et al., 2011; Wallace et al., 2019). Figures 3C–3F show examples of structures interpreted as dominantly tectonic, but we note that these features may overprint MTDs and/or include elements of drilling-induced deformation.

The hanging wall displays intervals of regularly spaced and locally pervasive fractures ≤100 m above the fault zone. These fractures are <5 mm thick, dip 20°–80°, and lack evidence for significant shear displacement (Fig. 3A). Hanging-wall bedding dips are 0°–50°, with variable dip directions recorded in logging-while-drilling

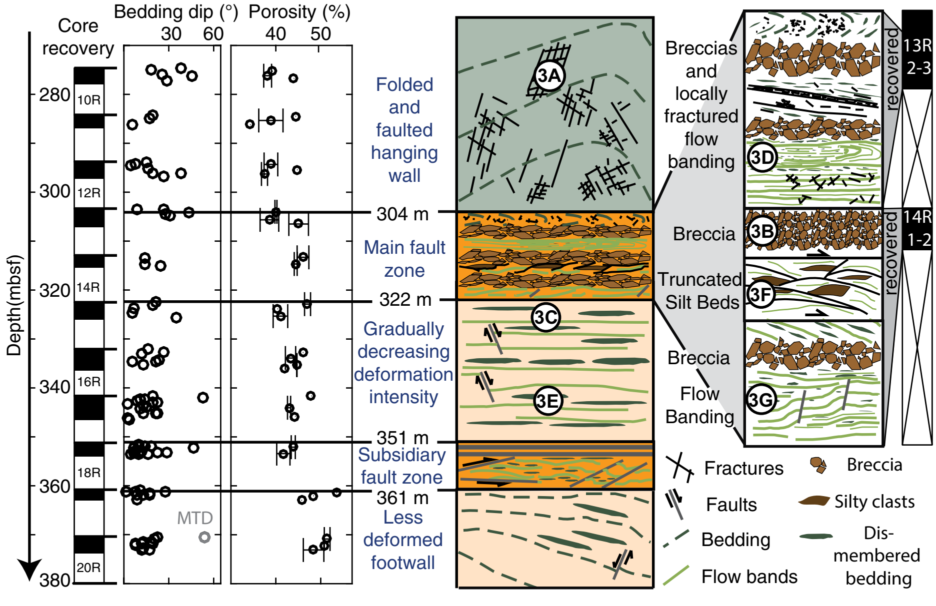

Figure 2. Summary schematic of fault zone structure at the Pāpaku fault (Hikurangi margin, New Zealand), compared to shipboard (core) bedding dip and porosity measurements, and with an indication of core recovery. Porosity is averaged by section of core, and error bars show one standard deviation. Key features of the fault zone include a fractured and folded hanging wall, breccias interlayered with ductilely sheared zones within the fault zone, and a relatively undeformed footwall. White circles indicate locations of photographs in Figure 3. MTD—mass transport deposit; mbsf—m below seafloor.

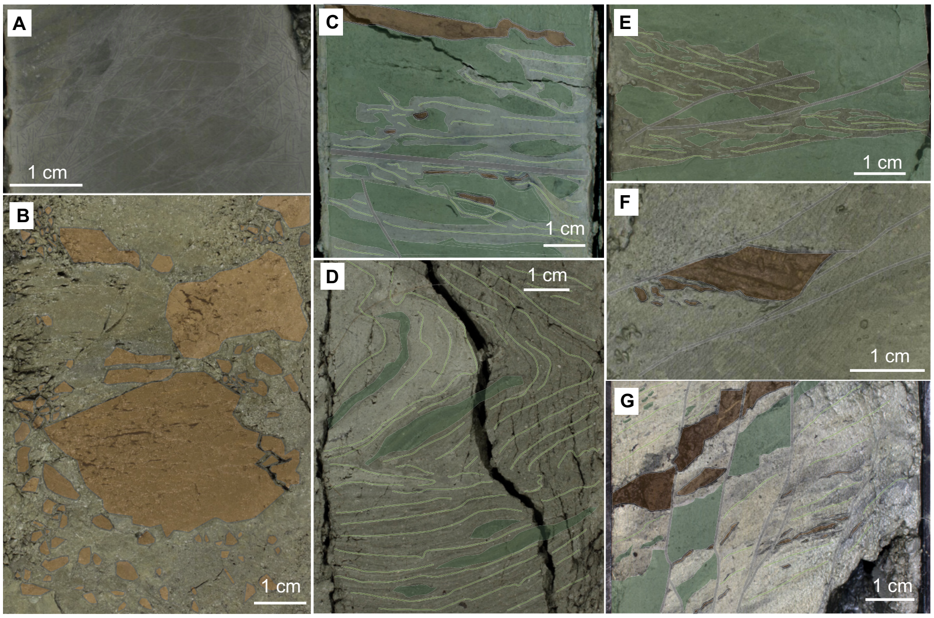

Figure 3. Representative deformation types within cores recovered from International Ocean Discovery Program (IODP) Expedition 375 Site U1518 (Pāpaku fault, Hikurangi margin, New Zealand) with transparent interpretational overlay following the legend in Figure 2. Separate clean photographs and interpretations are available in Figures DR1 and DR2 (see footnote 1). (A) Network of filled fractures in hanging-wall mudstone. (B) Breccia, mostly cohesive, although locally disaggregated into angular clasts. (C) Footwall-derived rocks showing ductile flow structures in mud containing more coherent clasts, including local injection features and faults. (D) Folded and intensely flow-banded and dismembered layers above the breccia shown in B. (E) Brittle-ductile deformation within a flow band in deformed footwall separating main and subsidiary faults. (F) Silty fragment bounded by faults, found immediately below breccia in B. (G) Example of less intensely flow-banded layers, comparable to stratal disruption, crosscut by normal faults.

(LWD) image logs, likely reflecting mesoscale folding (Fig. 2).

The top of the fault zone coincides with an ~0.5 m.y. biostratigraphic age inversion and is defined by a sharp transition from fractured and folded coherent bedding to brittlely and ductilely disrupted fault zone rocks, which are lithologically the same as the footwall sediments (Wallace et al., 2019). The top 18 m section of the fault consists of breccias tens of centimeters thick (Fig. 3B) separated by ductilely deformed intervals (Figs. 2 and 3D–3F). In parts of this 18 m interval, LWD image logs show disturbed bedding.

Breccias in the upper 18 m of the fault zone are ≤1 m thick, which represents a minimum thickness due to partial core recovery (Fig. 2). The breccias contain angular clasts up to a few centimeters long (Fig. 3B), lack lithologic layering, and are poorly cemented by a sedimentary fill. The combination of sedimentary fill (not drilling mud) and angular clast shapes is consistent with deformation below the seafloor, rather than during drilling or by gravity-driven sediment flow. It is possible that the breccias were further fragmented during drilling, but regardless, the fragmented fabric represents more brittle behavior at *in situ* conditions than in the intervening intervals preserving ductile flow banding (Figs. 3D–3G).

Locally, asymmetric clasts are bounded by faults (Figs. 3E and 3F), and flow bands are crosscut by faults that typically show normal offset (Figs. 3E and 3G). These relations between ductile and brittle structures show a dominance of faults crosscutting ductilely deformed layers (Figs. 3E and 3G). The faults are healed, typically by fine clays, and therefore predate drilling (which typically produces open, cohesionless fractures; Maltman, 1998). Consequently, the ductile features are interpreted as natural rather than drilling-induced. Neither breccias nor flow bands display intragranular fractures. Whereas flow bands are defined by a shape-preferred orientation of grains, breccias have locally aligned clast long axes, but their component sedimentary grains are not preferentially oriented (Fig. 3; Figs. DR3–DR5). The penetrative alignments are not continuous with drilling mud along the core liner or in pore spaces, nor are they arcuate records of rotary drilling, providing further evidence that they are not drilling-induced (Maltman, 1998).

At the base of the main fault, deformation intensity decreases gradually into the footwall, where ductile structures are more pervasive than fractures (Figs. 2, 3C, and 3E). A brittle-ductile subsidiary fault at 351–361 m below the seafloor (mbsf) marks the top of an essentially undeformed footwall with no associated change in lithotratigraphy or biostratigraphy (Fig. 2). The interval spanning the main and subsidiary faults (304–361 mbsf) features a subtle increase in average porosity, measured on comparatively coherent core samples, relative to the hanging wall. Beneath the subsidiary fault, porosity increases sharply to ~50%, as opposed to 40%–45% within the fault zone (Fig. 2).

FAULT ZONE DEFORMATION SEQUENCE

The ~60-m-thick Pāpaku fault zone consists of two high-strain zones separated by less-deformed sediments. Although we group the two faults and the material between them as “the fault zone,” we cannot differentiate whether the two faults formed simultaneously or represent imbricates formed at different times. The structures described here ignore those with drilling-induced characteristics (such as open and/or axially symmetric fractures, arcuate lineations, and interstitial drilling mud; Maltman, 1998) and gravity flow deposits with basal erosional surfaces, chaotic internal structure, and an upward-fining cover (Strasser et al., 2011). We therefore assume the structures have a dominantly tectonic origin related to the ~6 km of displacement on the Pāpaku fault. The microscale mechanism of shallow ductile deformation without intragrain fractures was granular flow, governed by frictional and fluid-flow properties that are sensitive to small stress perturbations in the low-stress (total and effective) environment of the sampled depths (Savage, 1984). We suggest two interpretations to explain the observation that mesoscale faults overprint ductilely deformed layering.

One interpretation arises from the observation that brittle deformation is preferred in the hanging wall, because it has been uplifted and unroofed and is overconsolidated for its current depth, whereas higher porosity in the footwall leads to the dominantly ductile deformation observed there (e.g., Zhang et al., 1993). The fact that the footwall-derived brittle-ductile fault has lower porosity than the footwall itself requires consolidation within the fault. Such consolidation is consistent with a progression from initial ductile to later brittle deformation during downward fault growth into footwall sediments (e.g., Moore and Byrne, 1987; Morgan and Karig, 1995).

It is equally possible that the fault zone experienced coeval or cyclic brittle-ductile deformation, as inferred along exhumed subduction thrusts (Rowe et al., 2011, 2013; Webber et al., 2018). If ductile deformation overprinted brittle structures, it is unlikely that the brittle structures would be preserved in a recognizable form. That the deformation modes were coeval is consistent with flow bands preserved between intensely brecciated intervals, without being affected by this brittle deformation.

MIXED-MODE DEFORMATION AND VARIATIONS IN FAULT SLIP STYLE

The Pāpaku fault exhibits mixed brittle-ductile deformation in an area of well-documented SSEs and tsunami earthquakes hosted on the plate interface and/or upper-plate faults (Bell et al., 2014; Wallace et al., 2016; Todd et al., 2018; Shaddox and Schwartz, 2019). The Nankai (Japan) and Costa Rica subduction margins also have well-documented shallow SSEs in regions sampled by drilling (Davis et al., 2015; Araki et al., 2017), and there is evidence for coseismic slip along shallow faults at the Nankai margin (Sakaguchi et al., 2011). In these areas, zones of ductilely deformed rocks were also reported; the base of the Costa Rica décollement has ductile clays (Tobin et al., 2001), and the Nankai plate interface includes meters-thick intervals of clay-rich sediments with scaly fabrics (Kinoshita et al., 2009). Deformation distributed over tens of meters in regions of mixed fault slip behavior including SSEs is therefore not a unique property of the Pāpaku fault (Rowe et al., 2013), although the fault differs in its lack of scaly clay fabric, and in the existence of co-located, intense, ductile flow fabrics and breccias.

At both the Nankai and northern Hikurangi margins, kilometers of plate convergence are accommodated on splay faults (Fig. 1B; Moore et al., 2007; Araki et al., 2017), which host low-frequency earthquakes (Obana and Kodaira, 2009; Shaddox and Schwartz, 2019). Although geodetic observations neither necessitate it nor rule it out, geological evidence for multiple deformation modes on the Pāpaku fault suggests that the geophysically observed low-frequency earthquakes are not its only active slip style. Time-variable behavior of shallow splays should therefore be considered in interpretation of SSEs and in seismic and tsunami hazard models.

Referring back to the three existing hypotheses for temporal and spatial variations in fault slip style, our direct observations of the Pāpaku fault show that

(1) Lithological heterogeneity is not the main reason for mixed brittle-ductile deformation within the Pāpaku fault, because lithological contrast is restricted to centimeter-scale variations that do not correlate with different structures.

(2) A displacement-dependent or time-dependent brittle-ductile transition is demanded by the progressive and coeval interpretations of the fault rock sequence, respectively. During granular flow at low effective stress, such a transition is consistent with temporal changes in loading rate (Savage, 1984), and associated transitions in frictional stability (Scholz, 1998; Ikari and Kopf, 2017; Leeman et al., 2018).

(3) Structures indicative of fluidization are locally present (e.g., Fig. 3C) and suggest that local and transient increases in pore fluid pressure can modulate slip mode.

In summary, the data from IODP Site U1518 suggest that the Pāpaku fault has experienced mixed styles of slip as a function of loading rate and/or pore fluid pressure, as documented by the varied brittle and ductile structures, and as allowed by the large displacement and low effective stress of the fault at the sampling site. The changes in loading rate and fluid pressure could, for example, arise from earthquakes that nucleate downdip of the drill site, stress changes from downdip SSEs, or pore-pressure transients related to strain-induced compaction or transient fluid pulses. These interpretations imply that shallow subduction thrusts in hemipelagic sediments are capable of a range of slip speeds, at different times, in the same location, because their frictional stability is highly sensitive to small stress perturbations.

ACKNOWLEDGMENTS

This research used samples and data provided by the International Ocean Discovery Program (IODP). We thank the staff onboard the RV *JOIDES Resolution* during IODP Expeditions 372 and 375 for their support. Fagereng is supported by European Research Council Starting Grant 715836, and Fagereng and Bell received funding from Natural Environment Research Council IODP Moratorium Grants NE/S002731/1 and NE/S00291X/1. Savage was supported by an award from the U.S. Science Support Program/International Ocean Discovery Program (National Science Foundation grant OCE-1450528). Barnes and Wallace were supported by the Endeavor fund, administered by New Zealand's Ministry for Business, Innovation, and Employment. Reviews by Christie Rowe and several anonymous reviewers significantly improved the manuscript.

REFERENCES CITED

Araki, E., Saffer, D.M., Kopf, A.J., Wallace, L.M., Kimura, T., Machida, Y., Ide, S., Davis, E., and IODP Expedition 365 Shipboard Scientists, 2017, Recurring and triggered slow-slip events near the trench at the Nankai Trough subduction megathrust: Science, v. 356, p. 1157–1160, https://doi.org/10.1126/science.aan3120.

Barker, D.H.N., Henrys, S., Caratori Tontini, F., Barnes, P.M., Bassett, D., Todd, E., and Wallace, L., 2018, Geophysical constraints on the relationship between seamount subduction, slow slip, and tremor at the north Hikurangi subduction zone, New Zealand: Geophysical Research Letters, v. 45, p. 12,804–12,813, https://doi.org/10.1029/2018GL080259.

Bell, R., Holden, C., Power, W., Wang, X., and Downes, G., 2014, Hikurangi margin tsunami earthquake generated by slow seismic rupture over a subducted seamount: Earth and Planetary Science Letters, v. 397, p. 1–9, https://doi.org/10.1016/j.epsl.2014.04.005.

Byrne, T., 1984, Early deformation in mélange terranes of the Ghost Rocks Formation, Kodiak Islands, Alaska, *in* Raymond, L.A., ed., Mélanges: Their Nature, Origin, and Significance: Geological Society of America Special Paper 198, p. 21–52, https://doi.org/10.1130/SPE198-p21.

Chester, F.M., et al., 2013, Structure and composition of the plate-boundary slip zone for the 2011 Tohoku-Oki earthquake: Science, v. 342, p. 1208–1211, https://doi.org/10.1126/science.1243719 .

Davis, E.E., Villinger, H., and Sun, T., 2015, Slow and delayed deformation and uplift of the outermost subduction prism following ETS and seismogenic slip events beneath Nicoya Peninsula, Costa Rica: Earth and Planetary Science Letters, v. 410, p. 117–127, https://doi.org/10.1016/j.epsl.2014.11.015.

Doser, D.I., and Webb, T.H., 2003, Source parameters of large historical (1917–1961) earthquakes, North Island, New Zealand: Geophysical Journal International, v. 152, p. 795–832, https://doi.org/10.1046/j.1365-246X.2003.01895.x.

Ikari, M.J., and Kopf, A.J., 2017, Seismic potential of weak, near-surface faults revealed at plate tectonic slip rates: Science Advances, v. 3, p. e1701269, https://doi.org/10.1126/sciadv.1701269.

Kinoshita, M., Tobin, H., Ashi, J., Kimura, G., Lallemant, S., Screaton, E.J., Curewitz, D., Masago, H., Moe, K.T., and Expedition 314/315/316 Scientists, 2009, NanTroSEIZE Stage 1: Investigations of seismogenesis, Nankai Trough, Japan: Proceedings of the Integrated Ocean Drilling Program, Volume 314/315/316: College Station, Texas, International Ocean Discovery Program.

Leeman, J.R., Marone, C., and Saffer, D.M., 2018, Frictional mechanics of slow earthquakes: Journal of Geophysical Research–Solid Earth, v. 123, p. 7931–7949, https://doi.org/10.1029/2018JB015768.

Liu, Y., and Rice, J.R., 2007, Spontaneous and triggered aseismic deformation transients in a subduction fault model: Journal of Geophysical Research, v. 112, B09404, https://doi.org/10.1029/2007JB004930.

Maltman, A.J., 1998, Deformation structures from the toes of active accretionary prisms: Journal of the Geological Society [London], v. 155, p. 639–650, https://doi.org/10.1144/gsjgs.155.4.0639.

Moore, G.F., Bangs, N.L., Taira, A., Kuramoto, S., Pangborn, E., and Tobin, H.J., 2007, Three-dimensional splay fault geometry and implications for tsunami generation: Science, v. 318, p. 1128–1131, https://doi.org/10.1126/science.1147195.

Moore, J.C., and Byrne, T., 1987, Thickening of fault zones: A mechanism of mélange formation in accreting sediments: Geology, v. 15, p. 1040–1043, https://doi.org/10.1130/0091-7613(1987)15<1040:TOFZAM>2.0.CO;2.

Morgan, J.K., and Karig, D.E., 1995, Décollement processes at the Nankai accretionary margin, southeast Japan: Propagation, deformation, and dewatering: Journal of Geophysical Research, v. 100, p. 15,221–15,231, https://doi.org/10.1029/95JB00675.

Obana, K., and Kodaira, S., 2009, Low-frequency tremors associated with reverse faults in a shallow accretionary prism: Earth and Planetary Science Letters, v. 287, p. 168–174, https://doi.org/10.1016/j.epsl.2009.08.005.

Rowe, C.D., Meneghini, F., and Moore, J.C., 2011, Textural record of the seismic cycle: Strain-rate variation in an ancient subduction thrust, *in* Fagereng, Å., et al., eds., Geology of the Earthquake Source: A Volume in Honour of Rick Sibson: Geological Society [London] Special Publication 359, p. 77–95, https://doi.org/10.1144/SP359.5.

Rowe, C.D., Moore, J.C., Remitti, F., and IODP Expedition 343/343T Scientists, 2013, The thickness of subduction plate boundary faults from the seafloor into the seismogenic zone: Geology, v. 41, p. 991–994, https://doi.org/10.1130/G34556.1.

Saffer, D.M., and Wallace, L.M., 2015, The frictional, hydrologic, metamorphic and thermal habitat of shallow slow earthquakes: Nature Geoscience, v. 8, p. 594–600, https://doi.org/10.1038/ngeo2490.

Sakaguchi, A., Chester, F., Curewitz, D., Fabbri, O., Goldsby, D., Kimura, G., Li, C.F., Masaki, Y., Screaton, E.J., Tsutsumi, A., and Ujiie, K., 2011, Seismic slip propagation to the updip end of plate boundary subduction interface faults: Vitrinite reflectance geothermometry on Integrated Ocean Drilling Program NanTro SEIZE cores: Geology, v. 39, p. 395–398, https://doi.org/10.1130/G31642.1.

Savage, S.B., 1984, The mechanics of rapid granular flows: Advances in Applied Mechanics, v. 24, p. 289–366, https://doi.org/10.1016/S0065-2156(08)70047-4.

Scholz, C.H., 1998, Earthquakes and friction laws: Nature, v. 391, p. 37–42, https://doi.org/10.1038/34097.

Screaton, E., Kimura, G., Curewitz, D., Moore, G., and IODP Expedition 316 Scientists, 2009, Interactions between deformation and fluids in the frontal thrust region of the NanTroSEIZE transect offshore the Kii Peninsula, Japan: Results from IODP Expedition 316 Sites C0006 and C0007: Geochemistry Geophysics Geosystems, v. 10, Q0AD01, https://doi.org/10.1029/2009GC002713.

Segall, P., Rubin, A.M., Bradley, A.M., and Rice, J.R., 2010, Dilatant strengthening as a mechanism for slow slip events: Journal of Geophysical Research, v. 115, B12305, https://doi.org/10.1029/2010JB007449.

Shaddox, H.R., and Schwartz, S.Y., 2019, Subducted seamount diverts shallow slow slip to the forearc of the northern Hikurangi subduction zone, New Zealand: Geology, v. 47, https://doi.org/10.1130/G45810.1.

Skarbek, R.M., Rempel, A.W., and Schmidt, D.A., 2012, Geologic heterogeneity can produce aseismic slip transients: Geophysical Research Letters, v. 39, L21306, https://doi.org/10.1029/2012GL053762.

Solomon, E.A., Huepers, A., Luo, M., Malie, P., Saffer, D.M., Torres, M.E., Wallace, L.M., Petronotis, K.E., Barnes, P., Pecher, I.A., LeVay, L., and Expedition IODP 375 and 372 Scientists, 2018, Geochemical constraints on fluid-rock reactions, fluid sources, and flow pathways along the IODP Expedition 375 transect; northern Hikurangi margin: Washington, D.C., American Geophysical Union, Fall meeting, abstract T54C–07.

Strasser, M., Moore, G.F., Kimura, G., Kopf, A.J., Underwood, M.B., Guo, J., and Screaton, E.J., 2011, Slumping and mass transport deposition in the Nankai fore arc: Evidence from IODP drilling and 3-D seismic reflection data: Geochemistry Geophysics Geosystems, v. 12, Q0AD13, https://doi.org/10.1029/2010GC003431.

Tobin, H., Vannucchi, P., and Meschede, M., 2001, Structure, inferred mechanical properties, and implications for fluid transport in the décollement zone, Costa Rica convergent margin: Geology, v. 29, p. 907–910, https://doi.org/10.1130/0091-7613(2001)029<0907:SIMPAI>2.0.CO;2.

Todd, E.K., Schwartz, S.Y., Mochizuki, K., Wallace, L.M., Sheehan, A.F., Webb, S.C., Williams, C.A., Nakai, J., Yarce, J., Fry, B., and Henrys, S., 2018, Earthquakes and tremor linked to seamount subduction during shallow slow slip at the Hikurangi margin, New Zealand: Journal of Geophysical Research, v. 123, p. 6769–6783, https://doi.org/10.1029/2018JB016136.

Wallace, L.M., and Beavan, J., 2010, Diverse slow slip behavior at the Hikurangi subduction margin, New Zealand: Journal of Geophysical Research, v. 115, B12402, https://doi.org/10.1029/2010JB007717.

Wallace, L.M., Beavan, J., McCaffrey, R., and Darby, D., 2004, Subduction zone coupling and tectonic block rotations in the North Island, New Zealand: Journal of Geophysical Research, v. 109, B12406, https://doi.org/10.1029/2004JB003241.

Wallace, L.M., Webb, S.C., Ito, Y., Mochizuki, K., Hino, R., Henrys, S., Schwartz, S.Y., and Sheehan, A.F., 2016, Slow slip near the trench at the Hikurangi subduction zone, New Zealand: Science, v. 352, p. 701–704, https://doi.org/10.1126/science.aaf2349.

Wallace, L.M., Saffer, D.M., Barnes, P.M., Pecher, I.A., Petronotis, K.E., LeVay, L.J., and Expedition 372/375 Scientists, 2019, Hikurangi subduction margin coring, logging, and observatories: Proceedings of the International Ocean Discovery Program, Volume 372B/375: College Station, Texas, International Ocean Discovery Program, https://doi.org/10.14379/iodp.proc.372B375.2019.

Webber, S., Ellis, S., and Fagereng, Å., 2018, "Virtual shear box" experiments of stress and slip cycling within a subduction interface mélange: Earth and Planetary Science Letters, v. 488, p. 27–35, https://doi.org/10.1016/j.epsl.2018.01.035.

Zhang, J., Davis, D.M., and Wong, T.-F., 1993, The brittle-ductile transition in porous sedimentary rocks: Geological implications for accretionary wedge aseismicity: Journal of Structural Geology, v. 15, p. 819–830, https://doi.org/10.1016/0191-8141(93)90178-D.

Printed in USA